Science of the Total Environment 644 (2018) 1160–1170

Contents lists available at ScienceDirect

Science of the Total Environment

journal homepage: www.elsevier.com/locate/scitotenv

Modelling glacier variation and its impact on water resource in the Urumqi Glacier No. 1 in Central Asia

Hongkai Gao [a,b,c,d], Hong Li [e,*], Zheng Duan [f], Ze Ren [g], Xiaoyu Meng [h,i], Xicai Pan [j]

[a] Key Laboratory of Geographic Information Science (Ministry of Education), East China Normal University, Shanghai, 200241, China
[b] School of Geographic Sciences, East China Normal University, Shanghai, 200241, China
[c] Key Laboratory for Mountain Hazards and Earth Surface Process, Institute of Mountain Hazards and Environment, Chinese Academy of Sciences, Chengdu, China
[d] Julie Ann Wrigley Global Institute of Sustainability, Arizona State University, Tempe, AZ 85287, USA
[e] The Norwegian Water Resources and Energy Directorate, Norway
[f] Hydrology and River Basin Management, Technical University of Munich, Arcisstrasse 21, 80333 Munich, Germany
[g] Flathead Lake Biological Station, University of Montana, Polson, MT 59860, USA
[h] Xinjiang Institute of Ecology and Geography, Chinese Academy of Science, Urumqi 830011, Xinjiang, China
[i] University of Chinese Academy of Science, Beijing 100039, China
[j] Fengqiu Agro-ecological Experimental Station, State Key Laboratory of Soil and Sustainable Agriculture, Institute of Soil Science, Chinese Academy of Sciences, Nanjing, China

HIGHLIGHTS

- A glacio-hydrology model (FLEX^G-Δh) is developed and validated in Urumqi Glacier No. 1 catchment, which is best monitored in China.
- In future, glacier area will likely lose up to 54% of their 1980 extent in 2050, 80% in 2100; ice volume will lose up to 79% in 2050, 92% in 2100.
- The tipping point (*peak water*) of glacier melt supply is projected to occur around 2020 and then runoff will decrease significantly.

GRAPHICAL ABSTRACT

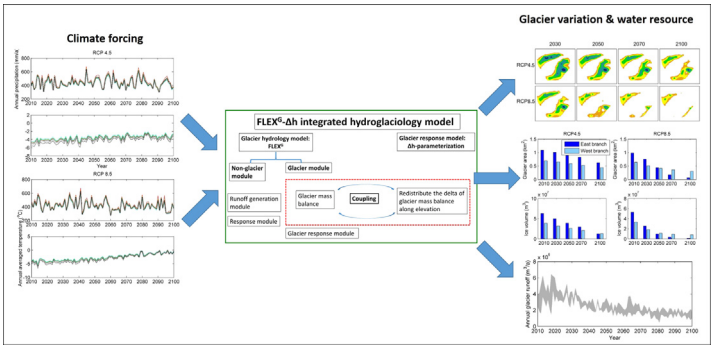

ARTICLE INFO

Article history:
Received 31 October 2017
Received in revised form 30 June 2018
Accepted 1 July 2018
Available online 11 July 2018

Keywords:
FLEX hydrological model
Glacier retreat model
China
Climate change
The Urumqi Glacier No. 1 catchment
Water resources

ABSTRACT

Climate warming is expected to accelerate glacier retreat and shift hydrological regime, which poses great threat to regional water resources in terms of amount, variability, and quality. This is especially true in arid regions with glaciers such as the Central Asia. However, few models manage to mimic both glacier runoff and surface changes with adequate performance. To narrow this gap, we integrated a spatially distributed hydrological model (FLEX^G) and a glacier retreat model (Δh-parameterization), and tested the new model in the Urumqi Glacier No. 1 catchment, which is best monitored in China. The model inputs include climate forcing, topographic map and initial ice thickness. Here we validated the model with runoff observation at downstream and glacier measurements, i.e. three historical glacier area maps (1980, 1994 and 2002), annual glacier mass balance (GMB) and equilibrium line altitude (ELA). Results show that the FLEX^G-Δh model performed well in estimating runoff (with Kling-Gupta efficiency 0.75 for hydrograph) and reproducing historical glacier area variation. Additionally the model generated reasonably spatial distribution of glacier thickness, which is important to examine glacier evolution at the Urumqi Glacier No. 1. Subsequently we ran the model forced by 12 combinations of two climate scenarios and six bias correction methods to assess the impact of climate change on glacier thinning, retreat, and its influence on water resource. The impact assessment shows that glacier area will lose up to a half (54%) of their 1980

* Corresponding author.
E-mail addresses: hkgao@geo.ecnu.edu.cn (H. Gao), holi@nve.no (H. Li), xicai.pan@issas.ac.cn (X. Pan).

https://doi.org/10.1016/j.scitotenv.2018.07.004
0048-9697/

extent in 2050, and up to 80% in 2100; while ice volume will decrease up to 79% in 2050, and 92% in 2100. The tipping point (*peak water*) of glacier melt supply was projected to occur around 2020 and then runoff would decrease significantly. These results alert us that there is a need for immediate mitigation measures to adapt to fast glacier change to assure long-term water security in this region.

1. Introduction

Meltwater from glaciers on high mountains is the lifeline for local and downstream residents, economy and ecosystems in the arid Central Asia (Ding et al., 2006; Immerzeel et al., 2010; Ren et al., 2017). Glaciers do not only provide valuable water, but they also act as important buffer against drought in dry seasons and years (Pritchard, 2017). Since glacier- and snowmelt are very sensitive to global warming (Huss et al., 2014), glaciers in most regions are experiencing accelerated melting, thinning, and retreating (Bhutiyani et al., 2008; Thayyen and Gergan, 2010; Immerzeel et al., 2012; Duethmann et al., 2014). This rises up huge risks to regional water resources, which are important to sustainable development of economy, society and environment (Immerzeel et al., 2010; Kraaijenbrink et al., 2017). Predicting glacier evolution and its impacts on hydrology is an urgent and critical question in practice as well as for scientific research.

Energy balance model is a physically based approach to calculate snow and ice melt by using energy fluxes to and from the snow/glacier surface (Wang et al., 2017). However, this approach requires many types of measurements, which in most cases is hardly available. Although various approaches has been proposed to derive energy components from conventional meteorological observation (Yang and Koike, 2005), the deriving processes would inevitably bring large uncertainty. Moreover, heterogeneous surface, e.g. debris cover, also substantially modify albedo, glacier melting and movement. Such high complexity hinders implementation of the energy balance approach into practice (Fujita and Sakai, 2014).

Temperature-index model is a relative simple approach by only using air temperature as a lumped index representing the energy budget (Zhang et al., 2007). Moreover, air temperature is one of the most conventional meteorological measurement and it has relatively constant relationship with elevation (lapse rate) allowing us to interpolate from in situ observation to spatial distribution (Wang et al., 2016). Therefore, the temperature-index model has been widely used in snow and glacier melting simulation in many regions around the globe (Matthews et al., 2015; Tarasova et al., 2016). A parameter, called a degree-day factor, which empirically links air temperature with snow and glacier melting, needs to be calibrated by observed data. Additionally, it is easy to extend the temperature-index model with other variables, e.g. albedo, shortwave radiation and topography (Gao et al., 2017a, 2017b).

Location of Glacier terminus and area are changing with climate. Therefore, coupling glacier dynamic into glacier hydrological model is necessary to assess glacier impacts of climate change on water

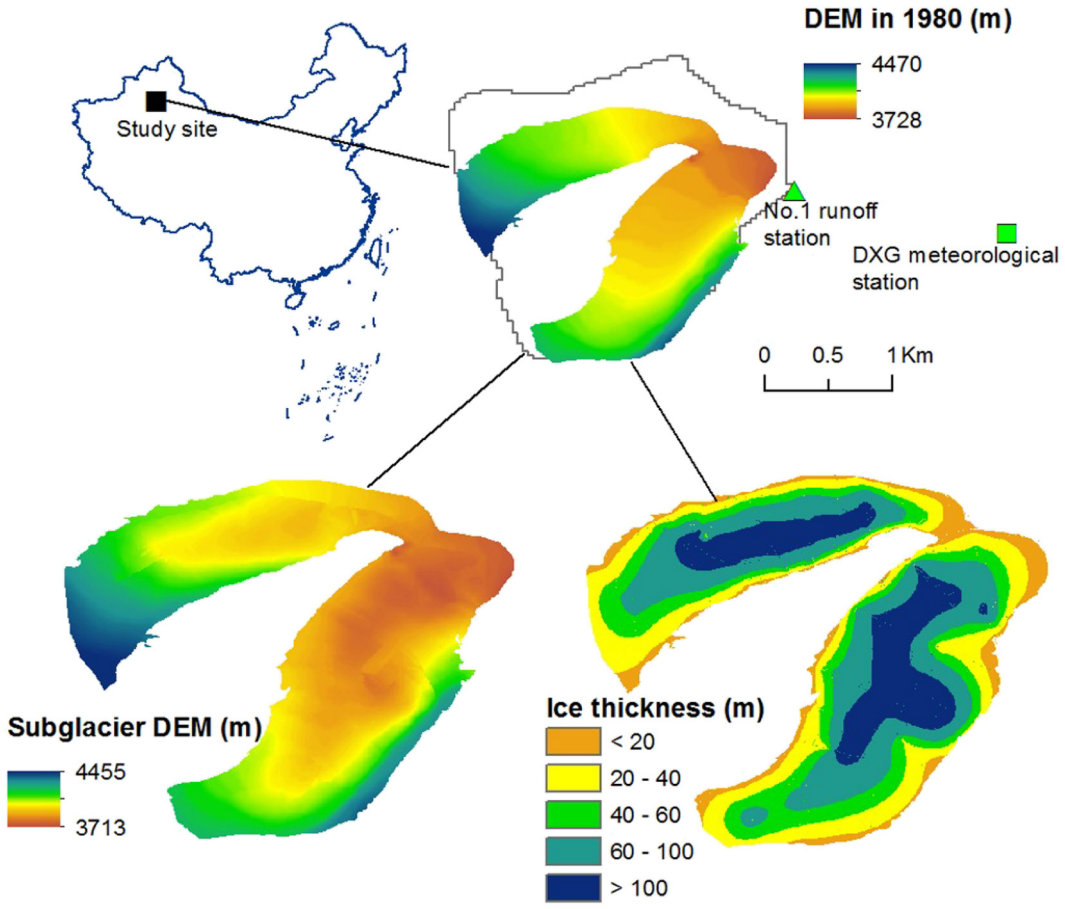

Fig. 1. The location of Urumqi Glacier No. 1, DEM, subglacial DEM, and ice thickness.

resources. However, simulating glacier responses is complicated, due to complex characteristics of ice, subglacial topography and roughness, and lack of data in glacier mountainous regions (Zhang et al., 2015).

Generally, there are two type approaches to simulate glacier dynamics, i.e. physically based ice flow models and empirical models. Physically based ice flow models considers the movement of glacier as viscous flow (Li et al., 2012; Zhang et al., 2015), described by Stokes equation, where ice movement is controlled by glacier geometry (e.g. length, slope, width and bed undulation) and ice characteristics (ice temperature and debris). This type of models needs tremendous amount of data, which limit its wide implementation, especially in ungauged basins. Moreover, the models based on the Stokes equation are expensive in terms of time and computing resources, which are not realistic in most cases. However, empirical models require less data and computing resources and they work well. For example, the area-volume model (Zhang et al., 2012) estimates the change of area by the change of ice volume, which approximately equals to the calculated glacier mass balance (GMB) assuming temporally stationary glacier area. This model can only estimate the change of glacier area in a lumped way, without spatial distribution information.

The Δh-parameterization approach (Huss et al., 2010; Li et al., 2015; Seibert et al., 2017) is another empirical approach to update the glacier surface elevation and area based on the simulated GMB from glacier hydrological model. The change of ice thickness in different elevations (Δh) is estimated based on its empirical parameterization with the normalized elevation range. The Δh-parameterization approach is developed from observed data in 34 glaciers in Switzerland, and used in many other glaciers in the world (Etter et al., 2017), but more vigorous test is still needed in Central Asia with long-term and in-situ multidisciplinary measurements.

Regarding the water resources from glacier, with temperature increasing, ice melting is accelerated resulting in the loss of glacier mass balance and the increase of melting water in the early stage. However, with the retreat of glacier, less glacier area contributes to melting water, leading to a decrease of water resources. Therefore, a "tipping point" exists which represents the peak of glacier melting water and

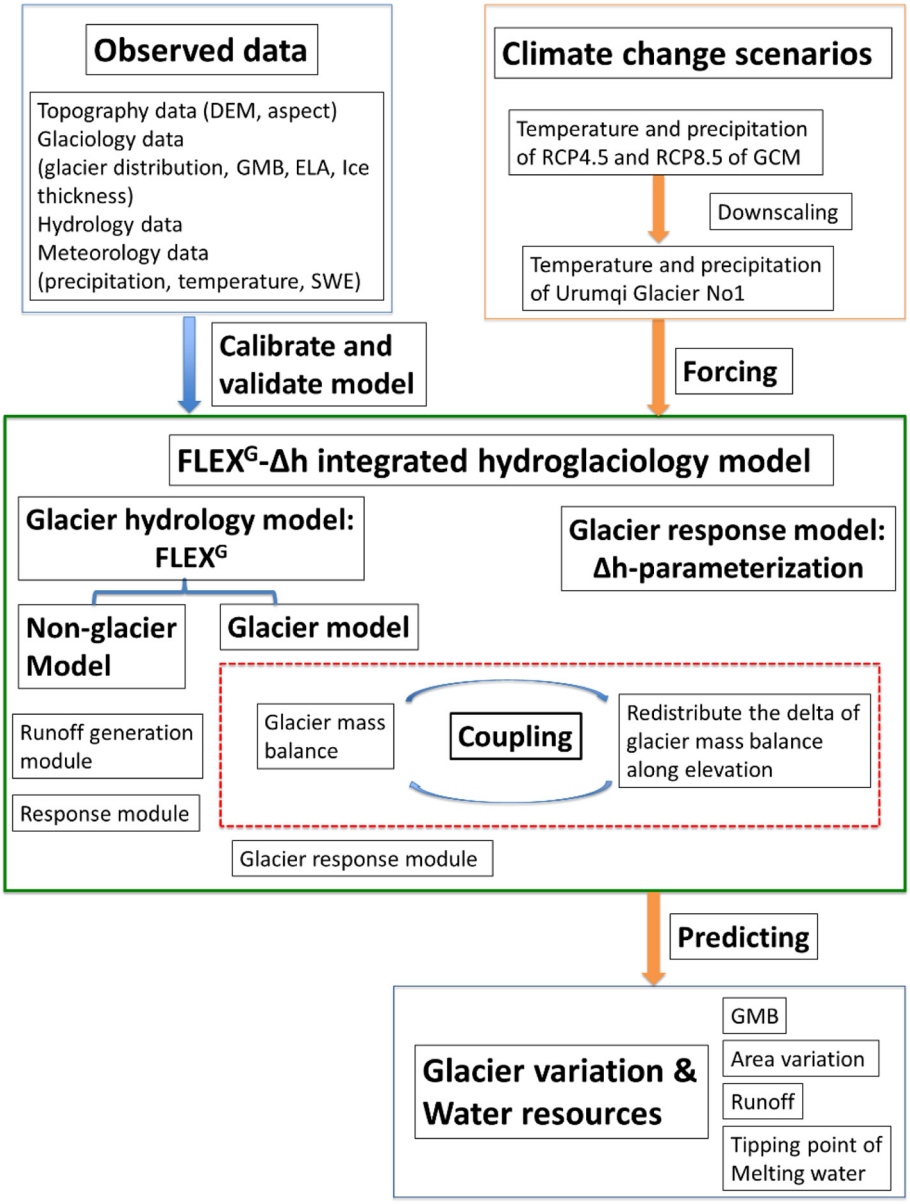

Fig. 2. The FLEX^G-Δ*h* modelling framework, and the work flow of model calibration, validation and predicting impacts of future climate change on glacier mass balance and glacier area, and melting water.

the turning point from the increase to decrease of melting water. Accurately predicting the tipping point is essential to make decisions on water resources management in the regions highly depending on glacier melt, to take measures to adapt to this change and assure long-term water security. This paper integrated a spatially distributed hydrological model (FLEX^G) and a glacier retreat model (Δh-parameterization), and tested the new model in the Urumqi Glacier No. 1 catchment.

Due to the harsh environment of the glacial and mountainous region in Central Asia, e.g. high altitude, lack of oxygen and ineffective transportation, continuous and long-term field measurement is extremely difficult. Lack of high quality in situ observation has been a bottleneck for glaciological and hydrological studies in this region. The Urumqi Glacier No. 1 has the longest glaciological observation in China, from 1959 to present (Ye et al., 2005), and with most comprehensive measurements including glaciology, meteorology, hydrology, topography, ecology and pedeology and geology variables and parameters. The Urumqi Glacier No. 1 provides us with a unique opportunity to understand the impact of climate change on glacier dynamic, to develop and validate glaciological and hydrological models, and to assess climate change impacts on water resources.

This paper is organized into five sections. In Section 2, we briefly introduced the study site – Urumqi Glacier No. 1 catchment, and the datasets used in this study including topography, glacier and hydrology data. Section 3 describes the methodology to couple a hydrological model (FLEX^G) with a glacier retreat model (Δh-parameterization). In Section 4, we presented the results to reproduce hydrograph, and glacier measurements, i.e. the historical variation of glacier area, GMB and ELA. Eventually we predicted the glacier response to future climate change and assessed its impact on water resources, especially the tipping point of glacier melt water. Finally, the conclusions drawn from this study were summarized in Section 5.

2. Study site and data

2.1. Study site and historical data

The Urumqi Glacier is located in the headwaters of the Urumqi River, in the Xinjiang Uyghur Autonomous Region in northwest China (43°50'N, 86°49'E; Fig. 1). The Urumqi Glacier became separated into two small dependent glaciers in 1994 and they are referred to east and west branch here. In 2002, the two branches covers respectively 1.12 and 0.72 km^2 and they lay between 3740 and 4490 m a.s.l. Daily runoff data from 1985 to 2004 was measured at the No. 1 gauge station, which lies 200 m downstream of the glacier terminus. The drainage area is 3.3 km^2 with 52% covered by glaciers. The rest area is bare soil/rock with sparse grass (Li et al., 2010).

Measurements of the Urumqi Glacier dates back to 1959 (Ye et al., 2005) and it is the longest measurement record of glaciers in China. The measurements include annual GMB and ELA (Dong et al., 2012). A missing period from 1967 to 1979 was reconstructed by meteorological data by Ye et al. (2005). Additionally, three photogrammetry respectively taken in 1980, 1994, and 2002 are available. The original maps are at a scale of 1:5000 and they are digitized to elevation surface model at a spatial resolution of 2.5 m. To setup the model, the initial ice thickness is interpolated from 679 measurements by radar taken in 1980. The weather forcing, daily temperature and precipitation are from the Da Xi Gou (DXG) station, which lies two kilometers from the

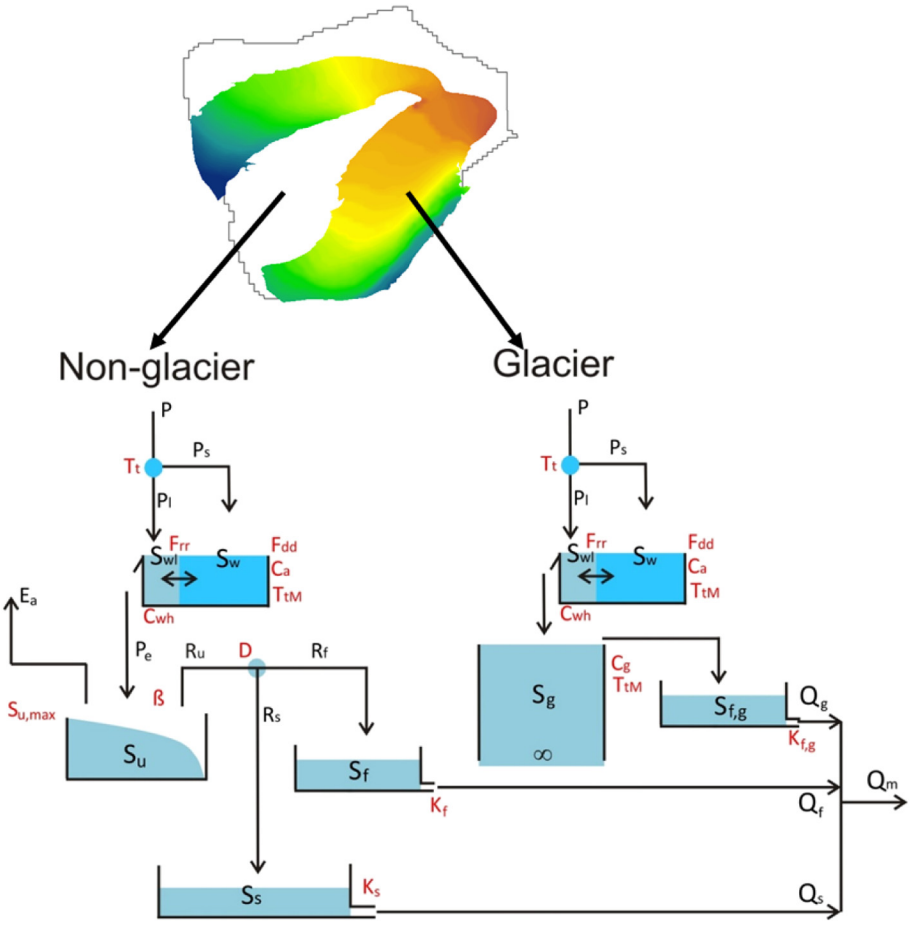

Fig. 3. Structure of the FLEX^G model. The red abbreviations indicate parameters, and black abbreviations indicate storage components and fluxes. The Δ*h*-parameterization method updates glacier area and surface elevation.

Table 1
The equations in FLEX^G model.

	Equations	Remarks
Precipitation phase separation	$P_s = \begin{cases} P; & T \le T_t \\ 0; & T > T_t \end{cases}$ (1) $P_l = \begin{cases} P; & T > T_t \\ 0; & T \le T_t \end{cases}$ (2)	Precipitation is considered to be snow (P_s) or rain (P_l) depending on whether the daily average air temperature (T) is above or below a threshold temperature, T_t [°C] (Eqs. (2), (3)).
Snow melt	$\frac{dS_w}{dt} = P_s + R_{rf} - M_s$ (3) $\frac{dS_{wl}}{dt} = P_l + M_s - R_{rf} - P_e$ (4) $M_s = \begin{cases} F_{dd} C_a (T - T_t); T > T_t \\ 0; \quad T \le T_t \end{cases}$ (5) $P_e = \begin{cases} S_{wl} - C_{wh} S_w; S_{wl} > C_{wh} S_w \\ 0; \quad S_{wl} \le C_{wh} S_w \end{cases}$ (6) $R_{rf} = \begin{cases} F_{dd} C_a F_{rr} (T - T_t); T_t > T \\ 0; \quad T_t \le T \end{cases}$ (7)	S_w is the solid snow pack, and S_{wl} is the liquid water inside the snow pack. R_{rf} (mm d^{-1}) is the refreezing water from liquid storage to solid storage. M_s (mm d^{-1}) indicates the melted snow. P_e (mm d^{-1}) is the generated runoff to soil/ice surface. Degree-day factor F_{dd} (mm °C^{-1} d^{-1}). melting threshold temperature T_t (°C). The influence of aspect is taken into account by a multiplier C_a (−). The F_{dd} in south facing aspects are multiplied by C_a, and the north facing aspects are multiplied by $1/C_a$, and the east/west facing aspects are kept as F_{dd}. fraction, C_{wh} (−), of the solid snow water equivalent (S_w). F_{rr} (−) indicates the correct factor to simulate liquid water refreezing, while temperature is below T_t.
Glaicer melt	$M_g = \begin{cases} F_{dd} C_a F_g (T - T_{tM}); T > T_{tM} \& S_w = 0 \\ 0; \quad T \le T_{tM} \text{ or } S_w > 0 \end{cases}$ (8) $\frac{dS_{f,g}}{dt} = P_l + M_g - Q_{f,g}$ (9) $Q_g = S_{f,g}/K_{f,g}$ (10)	M_g (mm d^{-1}) is glacier melt. The degree-day factor for glaciers is assumed to be larger than the snow degree-day factor for snow in the same region. This was here accounted for by the multiplier C_g. M_g is then, together with P_l routed through a linear reservoir $S_{f,g}$, controlled by a recession parameter $K_{f,g}$ (d), to compute the runoff generated from glacier areas
Non-glacier	$\frac{dS_u}{dt} = P_e - E_a - R_u$ (11) $\frac{R_u}{P_e} = 1 - (1 - \frac{S_u}{(1+\beta) S_{u,\max}})^{\beta}$ (12) $E_a = E_0 \frac{S_u}{C_e S_{u,\max}}$ (13) $\frac{dS_f}{dt} = R_f - Q_f$ (14) $\frac{dS_s}{dt} = R_s - Q_s$ (15) $Q_f = S_f/K_f$ (16) $Q_s = S_s/K_s$ (17)	P_e (mm d^{-1}) is the effective rainfall, i.e. snow melt and rainfall; E_a (mm d^{-1}) is the actual evaporation, which was estimated based on potential evaporation (E_0) and relative soil moisture ($S_u/S_{u,\max}$), with a free parameter C_e (−). R_u (mm d^{-1}) is the water that exceeds the storage capacity and cannot be stored in S_u. $S_{u,\max}$ (mm) is the root zone storage capacity and β (−) is the shape parameter. Excess water from S_u, i.e. R_u, recharges two linear reservoirs (S_f and S_s) as (R_f and R_s) by a parameter (D) to represent the response processes of subsurface storm flow Q_f (mm d^{-1}) and groundwater runoff Q_s (mm d^{-1}). K_f (d) is the fast recession parameter; and K_s (d) is the slow recession parameter.

discharge catchment. The climate is spatially distributed over the catchment with elevation adjust and more details are given in Section 3.1.1.

2.2. Future climate

Future climate data were produced by two steps. First, Global Climate Models (GCMs) were used to generate the future climate at the global scale and a sparse spatial resolution under certain assumptions about greenhouse gases (GHGs) emissions and changes in land use/land cover, etc. Second, the future climate is subsequently downscaled by Regional Climate Models (RCMs) and/or statistical methods to account for temporal and spatial variability in topography and vegetation. In the CORDEX datasets (accessed in September 2017), there are two domains covering the study area (East Asia and West Asia). We selected the model runs, which has historical and future climate runs for both temperature and climate. The HIRHAM 5 was forced by ICHEC-EC-EARTH with two emission scenarios (RCP4.5 and RCP8.5, which responses respectively to relative low and high GHGs emission) for the period of 2010–2100. However, there are certain bias existing in outputs from RCMs. The bias correction is to remove the discrepancy between outputs from climate model and observations from observations. There is an assumption that the bias for historical period and for the future are the same. The bias correction methods find a regression function between the discrepancy for the historical period and use the regression function to correct the future.

Table 2
Formulas of seven statistical bias correction methods.

Method (short)	Formula
M1 (empirical)	Empirical quantiles
M2 (splines)	Smoothing splines
M3 (linear)	$\widehat{p_o} = a + b \times p_m$
M4 (power.x)	$\widehat{p_o} = b \times (p_m - x)^c$
M5 (scale)	$\widehat{p_o} = b \times p_m$
M6 (power)	$\widehat{p_o} = b \times p_m^c$

Note: $\widehat{p_o}$ is estimation at observation site. p_m is the RCM modelled value. a, b, c, x and τ are free parameters that are estimated from station observation and historical RCM runs.

3. Methodology

The integrated modelling framework of FLEX^G and Δh is presented as Fig. 2. In this framework, glacier mass balance (GMB) is the bond linking the glacier melting module in FLEX^G and the Δh-parameterization method which redistributed the estimated GMB to different elevations. The calculated GMB by FLEX^G is the input for Δh-parameterization. Δh-parameterization redistributes the estimated GMB to different elevation bands, based on the empirical curves depending on the size of glaciers (Huss et al., 2010). The updated GMB by Δh-parameterization is used to update the glacier area and ice thickness, which are important input data for the FLEX^G model. Therefore, integrating the non-glacier hydrological model, the FLEX^G-Δh hydroglaciology model is developed.

Topographic (e.g. DEM and aspect) and meteorological data are important input for the FLEX^G-Δh model. And the glaciology data and hydrology data are used to calibrate and validate the model. Temperature and precipitation forcing of the RCP4.5 and RCP8.5 in the Urumqi Glacier No. 1 catchment were obtained by downscaling several GCMs. Bias correction methods were used to correct the estimated temperature and precipitation. With the FLEX^G-Δh model, future glacier variation and water resources were predicted. The future change of GMB, glacier area, runoff, and the tipping point of melting water were estimated by the modelling framework.

3.1. FLEX^G hydrological model

FLEX^G is a glacier hydrological model, integrated snow and glacier accumulation and ablation processes (Gao et al., 2012, 2017a). In this model, we classified the entire catchment into glacier and non-glacier regions, using the temperature-index approach aided by topographic data to calculate glacier runoff, and the Xin'anjiang storage capacity curve to calculate the runoff generation in non-glacier area (Fig. 3 shows the model structure, and essential equations with explanations in this model are summarized in Table 1.

3.1.1. Forcing data distribution

To account for influence of elevation on precipitation and temperature, the catchment was divided into 50 m elevation zones, resulting

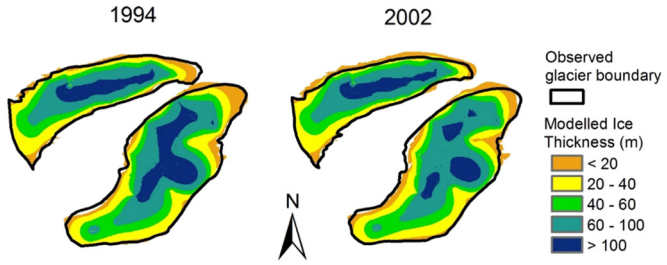

Fig. 4. Observed and simulated glacier boundary in 1994 and 2002.

in 16 elevation zones. Since there was only one meteorological station in this study site, but we need distributed forcing input to drive the FLEX^{G}-Δh model. A linear distribution method was applied to generate distributed forcing. The distributed temperature and precipitation for each elevation range were generated by interpolating the station observation at DXG meteorological station (3539 m). Temperature is linearly decreased with elevation, with a lapse rate of −0.007 °C m^{-1} (Gao et al., 2017a), and precipitation is linearly increased with elevation with a locally suitable lapse rate of 0.065% m^{-1} (Yang et al., 1988).

3.1.2. Snow melting

Precipitation is snow or rain depending on whether the daily average air temperature is below or above a threshold temperature (Eqs. (1) and (2) in Table 1). Due to systematic errors in snowfall measurement (Goodison et al., 1997; Yang et al., 2001), snowfall was adjusted with a lumped bias-correction factor of 1.3 (Yang et al., 1988). Snowpack was conceptualized as a porous media, which could hold liquid water from melting/rainfall and the liquid water can refreeze. In the temperature-index based snow model, Snowmelt was calculated on basis of a degree-day factor F_{dd} (mm °C^{-1} d^{-1}). This parameter was also impacted by aspect (Eq. (5)). Therefore, each elevation zone was further divided into three aspect zones, i.e. north (315–45°), south (135–225°) as well as the east/west (45–135° and 225–315°) facing aspects.

3.1.3. Glacier melting

The glacier component is also based on a temperature-index method (Eq. (8) in Table 1). The glacier only begins to melt when the ice is free of snow cover. Note that the degree-day factor for glaciers is assumed to be larger than the snow degree-day factor for snow in the same region (Seibert et al., 2015), mainly due to the lower albedo of ice than snow. This was here accounted for by the multiplier C_g. M_g is then, together with P_l routed through a linear reservoir $S_{f,g}$, controlled by a recession parameter $K_{f,g}$ (d), to compute the runoff generated from glacier areas (Eqs. (9), (10) in Table 1). Annual GMB of the entire Urumqi Glacier No. 1 estimated by the accumulation of glacier and snow pack simulations in individual elevation. Similarly, the annual ELA was derived by the annual GMBs of individual elevation zones, where the annual GMB is zero.

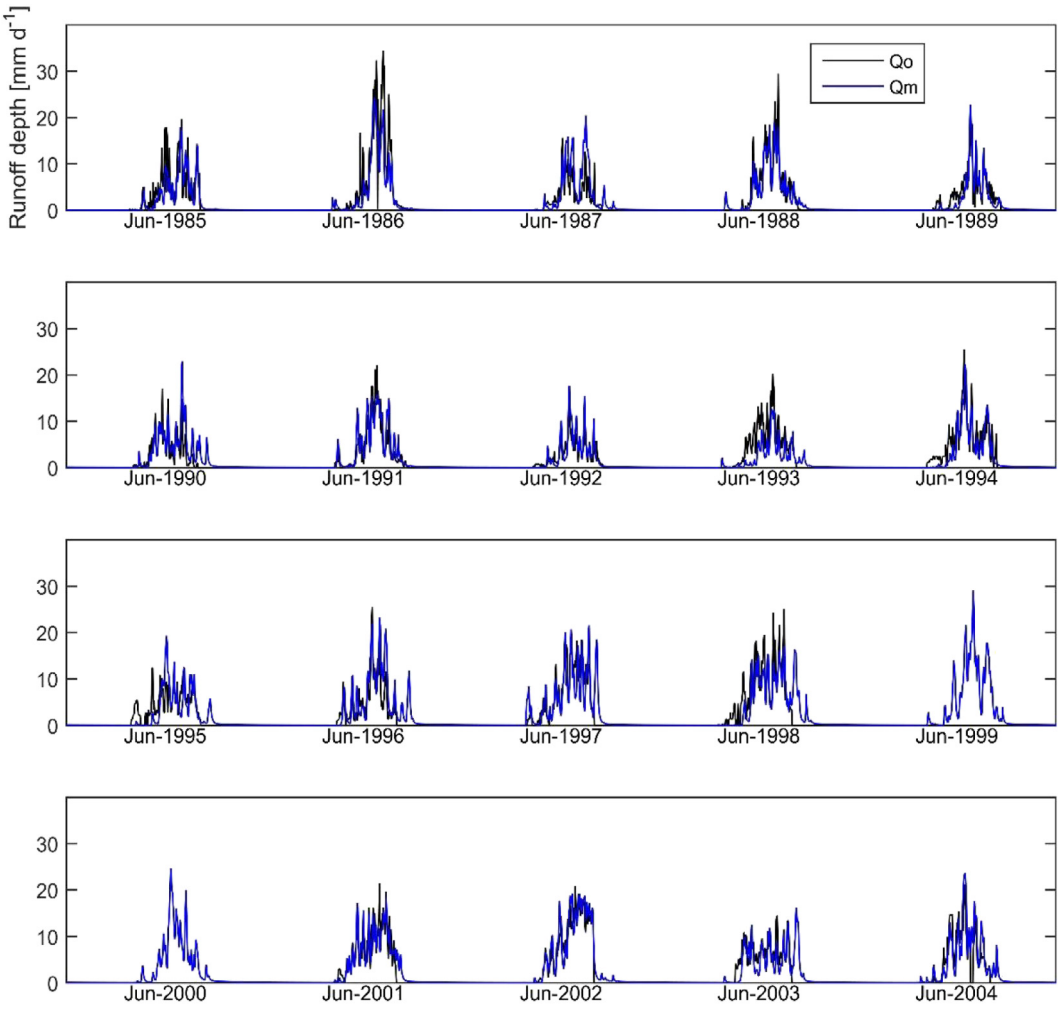

Fig. 5. Hydrograph at Glacier No. 1 station by the FLEX^{G}-Δ*h* model.

Table 3
Model performance for hydrograph and glacier measurements.

Calibration by I_{KGE}				Model evaluation by other criteria					
I_{KGE_HG}	I_{KGE_H} in calibration	I_{KGE_GMB}	I_{KGE_ELA}	I_{KGE_H} in validation	I_{r_GMB}	I_{r_ELA}	I_{BIAS_H} (mm/d)	I_{BIAS_GMB} (mm/a)	I_{BIAS_ELA} (m)
0.66	0.75	0.33	0.31	0.73	0.74	0.48	−0.54	−148	42

3.1.4. Non-glacier runoff modelling

Rainfall and snowmelt entered an unsaturated reservoir. Runoff generation is estimated based on relative soil moisture ($S_u/S_{u,max}$) and water input to the soil (Eq. (12) in Table 1), while actual evaporation is estimated based relative soil moisture and potential evaporation following Eq. (13) in Table 1 (Seibert, 1997). Excess water from S_u, i.e. R_u, recharges two linear reservoirs (S_f and S_s) by a parameter (D) to represent the response processes of subsurface storm flow Q_f and groundwater runoff Q_s (Eqs. (14) and (15) in Table 1), controlled by the fast recession parameter K_f and the slow recession parameter K_s (Eqs. (16) and (17) in Table 1).

3.2. Δh-parameterization

The Δh-parameterization is an empirical approach to allocate the change of GMB to different elevations (Huss et al., 2010). This method was proposed based on the long-term DEM observation in 34 glaciers in the Switzerland. Δh-parameterization used an empirical curve to simulate the change of ice thickness by their elevations. Conceptually, the locations with low elevation have large mass balance loss, and the locations in high altitude is not sensitive to the mass balance loss in low altitude. Although it is not physically-based, it is able to reproduce glacier retreat in diverse glacierized catchments. Delta-parameterization classified glaciers into three categories based on size, e.g. large valley glaciers (area > 20 km^2), medium valley glaciers (5km^2 < area < 20 km^2), and small glaciers (area < 5 km^2). We used the equation for small glacier in the Glacier No. 1 (less than 5 km^2).

$$\Delta h = (h_r - 0.30)^2 + 0.60(h_r - 0.30) + 0.09 \quad (18)$$

where Δh is the normalized surface elevation change and h_r is the normalized elevation range. Based on this equation, we updated the glacier elevation and surface every 5 years, to avoid some high frequency variation, because the Δh-parameterization is designed only for glacier retreat simulation.

3.3. Model calibration and validation

There are 13 free parameters in the FLEX^G-Δh model need to be calibrated. The prior ranges of parameter sets are kept the same as previous research (Gao et al., 2017a). A Monte-Carlo sampling strategy with 10^5 realizations from uniform prior parameter distributions was chosen to obtain posterior distributions for the period 1985–1994. The Kling-Gupta efficiency for streamflow (Gupta et al., 2009; I_{KGE}) was used as metric to evaluate model performance:

$$I_{KGE} = 1 - \sqrt{(r-1)^2 + (\alpha-1)^2 + (\beta-1)^2} \quad (19)$$

Where r is the linear correlation coefficient between simulation and observation; α (α = α_m/α_o) is a measure of relative variability in the

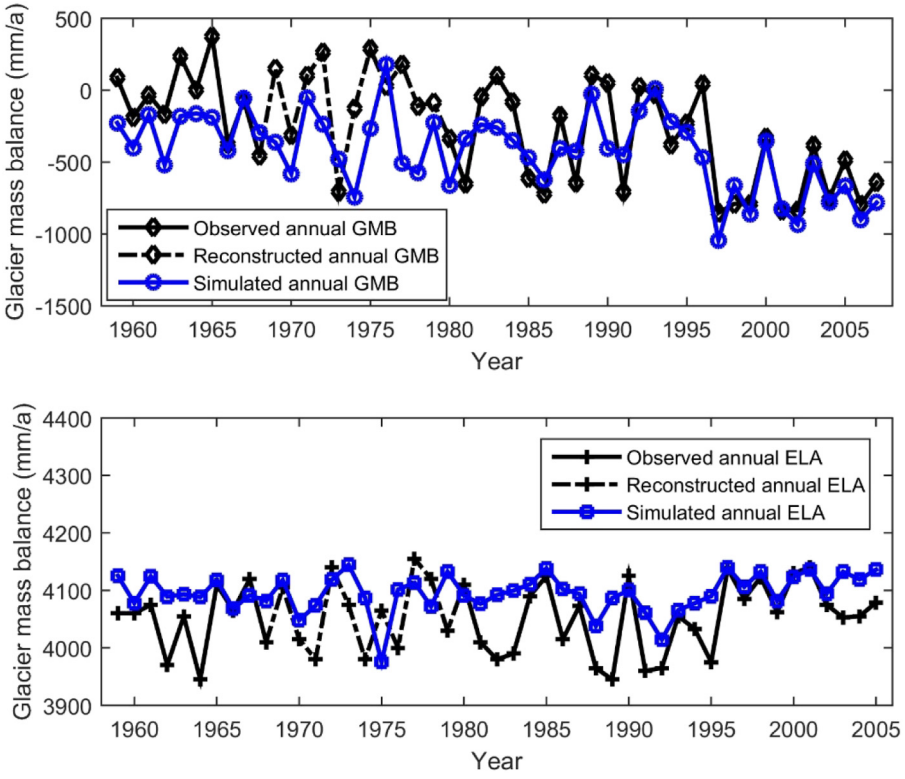

Fig. 6. Upper panel shows the modelled and observed glacier mass balance (GMB). Lower panel shows modelled and observed equilibrium line altitude (ELA). Dashed lines represent the GMB and ELA reconstructed from meteorological data from 1967 to 1979.

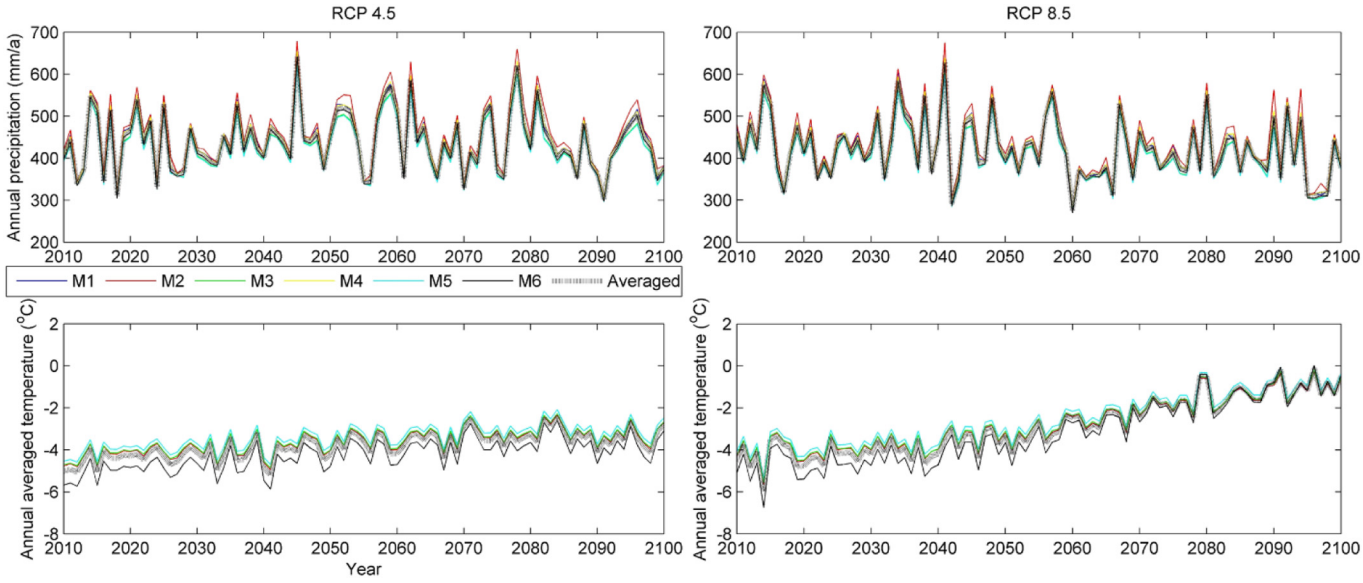

Fig. 7. The future change of air temperature and precipitation in the scenarios of RCP4.5 and RCP8.5, with six different bias correction methods.

simulated and observed values, where σ_m is the standard deviation of simulated runoff, and σ_o is the standard deviation of observed runoff; β is the ratio between the average value of simulated and observed data. Besides the hydrograph, ice accumulation and ablation are essential components of model system. Therefore, the weighted sum was used as the objective function (I_{KGE_HG}), to combine the three components into one metric, giving different weights to runoff (I_{KGE_H}), GMB (I_{KGE_GMB}), and ELA (I_{KGE_ELA}):

$$I_{KGE\_HG} = 0.8I_{KGE\_H} + 0.1I_{KGE\_GMB} + 0.1I_{KGE\_ELA} \quad (20)$$

We select weightage factors as 0.8, 0.1 and 0.1. Specifically the simulation of hydrography was given the highest weight, because the runoff data has 20-year time series in daily scale, as compared to the much lower temporal resolution of available GMB and ELA data. More importantly, we found the 0.8, 0.1 and 0.1 weightage factors perform better in hydrograph validation, which is a more rigorous model test (SI Table 1). The 1% best performing parameter sets were retained as behavioral and used to establish feasible posterior distributions and to construct model uncertainty ranges, using I_{KGE_HG} as informal likelihood measure (GLUE; Beven and Binley, 1992). The historical glacier area maps and the extra runoff dataset (1995–2004) were used to validate the FLEX^G-Δh model.

3.4. Future climate

RCMs outputs have certain bias and it is important to reduce the bias from the RCMs results. The most popular approaches are statistical transformations that adjust the probability distribution of modelled results to resemble observations. Here we used seven empirical bias correction methods (Gudmundsson et al., 2012), as shown in the Table 2. The bias correction methods have several parameters, which are determined by calibration. The calibration period for the bias corrections models are from 1959 to 2005, which is overlapping period of station observations and historical RCMs runs. The parameters values were used to bias correct the future climate scenarios with assumed GHGs emission scenarios (RCP4.5 and RCP8.5).

4. Results and discussion

4.1. Reproducing historical hydrograph and glacier variation

Fig. 4 shows the observed and the modelled glacier area extent in 1994 and 2002. We found that the FLEX^G-Δh model has the ability to reproduce glacier area variation. The simulated glacier area change of 1994–1980, 2002–1994, and 2002–1980 were 0.031km^2, 0.099 km^2 and 0.130 km^2, which were comparable with the observed area change,

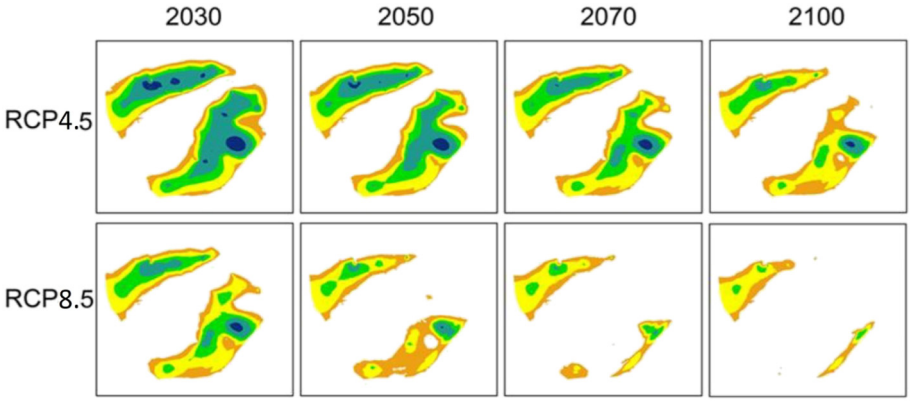

Fig. 8. The predicted glacier area changes in 2030, 2050, 2070 and 2100 in the scenarios of RCP4.5 and RCP8.5, with the averaged values of six different bias correction methods.

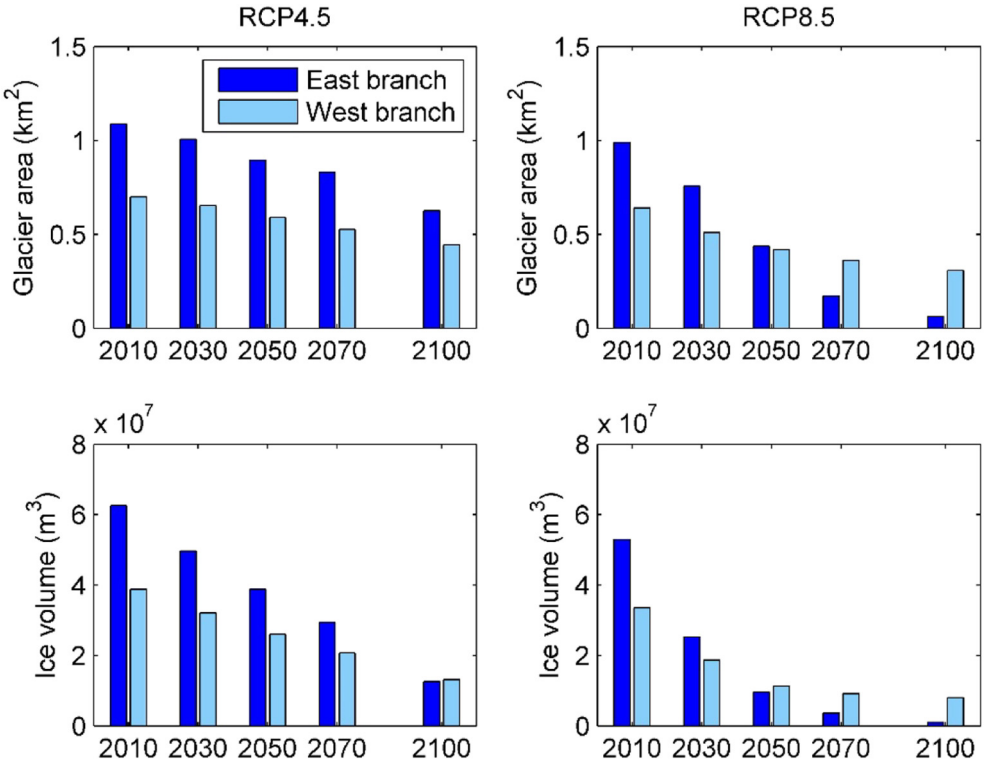

Fig. 9. Glacier area and ice volume changes from 2010 to 2100 in the climate scenarios of RCP 4.5 and RCP 8.5.

i.e. 0.038km^2, 0.113 km^2 and 0.151 km^2. Interestingly, in 1994 the west and east branches of the Glacier No. 1 were separated, which was well captured by the FLEX^G-Δ*h* model. This indicates the robustness of the FLEX^G-Δ*h* model to simulate glacier retreat. Fig. 4 also shows the shrinking of Glacier No. 1 for both east branch and west branch, which is qualitatively comparable with field measurements. Moreover, the maps represent the thinning of the Urumqi Glacier No. 1, which is largely in line with the long-term GMB observation.

The performance of the FLEX^G-Δh model to reproduce hydrographs of the Glacier No. 1 runoff gauge station is shown in Fig. 5 and Table 3. The simulated hydrograph is the averaged value generated by all the behavioral parameter sets. The I_{KGE} are 0.76 and 0.73 for calibration (1985–1994) and validation (1995–2004), respectively, which indicates the desirable performance of the FLEX^G-Δ*h* model. Moreover, the I_{KGE} of annual GMB and ELA are 0.33 and 0.31 respectively, with biases of -148 mm and 42 m. For annual details, Fig. 6 illustrates the capability of the FLEX^G-Δ*h* model to reproduce annual GMB and ELA in this glacierized catchment. Although the model reproduced the GMB and ELA quite well from 1985 on, the systematic underestimation of GMB and overestimation of ELA before 1985 likely indicates the effect of a decreasing glacier albedo due to dust accumulation in this region (Ming et al., 2013), or the neglecting of possible snow redistribution caused by the blowing snow from nonglacier areas to the glacier covered area, which likely influences on GMB and ELA (Schirmer et al., 2011). However, the lack of long-term albedo and snow redistribution observation prevents a meaningful parameterization of this process in the FLEX^G-Δh model.

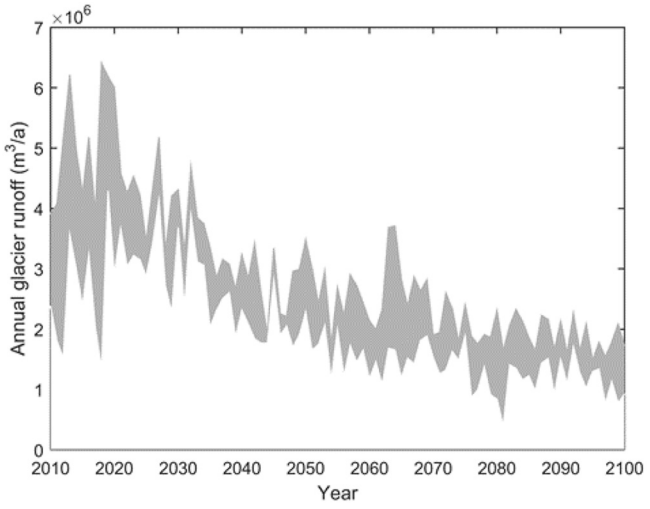

Fig. 10. The predicted annual glacier runoff of Urumqi Glacier No. 1 from 2010 to 2100. The gray areas indicates the uncertainty caused by different climate change scenarios of RCP4.5 and RCP8.5.

The ability to reproduce the historical glacier retreat maps and simultaneously fit the hydrographs proves the robustness of FLEX^G-Δh model, which allows us to further extend it to predict glacier variation and hydrology in future.

4.2. Predicting glacier retreat and melting water

4.2.1. Future climate change

Fig. 7 shows the predicted climate change by six different bias correction methods from 2010 to 2100. Interestingly, we found that six different bias correction methods perform very similar. This indicates the robustness of downscaling approaches, and the uncertainty of downscaling is small. The manifest difference between RCP4.5 and RCP8.5 indicates that different scenarios will result in quite different precipitation and temperature changes in future.

Precipitation (Fig. 7) varies without clear trends in both RCP4.5 and RCP8.5 scenarios. Temperature is increasing in both RCP4.5 and RCP8.5. In RCP4.5 scenario, the amount of annual precipitation decreases 0.26 mm/a, and annual average air temperature increases 0.017 °C/a. In RCP8.5 scenario, annual precipitation decreases 0.68 mm/a, and annual air temperature increases 0.038 °C/a. Generally, both scenarios

will experience decrease in precipitation and increase in air temperature, but the RCP8.5 scenario has much faster changes.

4.2.2. Glacier retreat and mass loss

With the forcing of future climate scenarios, we used the calibrated and validated FLEX^G-Δh model, with averaged behavioral parameters generated by GLUE, and calculated the glacier area and ice volume variation from 2010 to 2100 (Figs. 8, 9). It was found that under both climate change scenarios, both east and west branches of Glacier No. 1 exhibit a trend of retreating, area shrinkage and ice volume loss. However, different scenarios of climate change have massive difference, meaning that climate plays an essential role in glacier dynamics.

Quantitatively, in 1980 (the starting time of calculation), the area of east branch glacier is 1.14 km^2 and west branch glacier is 0.73km^2. Moreover, the ice volume of east branch glacier in 1980 is 7.13*$10^7$$m^3$, 4.33*$10^7$$m^3$ for west branch.

In the RCP4.5 scenario (Figs. 8, 9), the east branch shrinks to 1.09 km^2 (95%), 1.01 km^2 (88%), 0.90 km^2 (78%), 0.83 km^2 (73%), 0.63 km^2 (55%) in 2010, 2030, 2050, 2070 and 2100. Correspondingly, the ice volume shrinks to 6.26*10^7 m^3 (88%), 4.96*10^7 m^3 (70%), 3.88*10^7 m^3 (54%), 2.94*10^7 m^3 (41%), and 1.25*10^7 m^3 (18%). The area of west branch glacier shrinks to 0.70 km^2 (96%), 0.65 km^2 (90%), 0.59 km^2 (81%), 0.53 km^2 (72%), and 0.44 km^2 (61%) respectively in 2010, 2030, 2050, 2070 and 2100. Respectively, the volume of ice of the west branch glacier shrinks to 3.88*10^7 m^3 (90%), 3.21*10^7 m^3 (74%), 2.60*10^7 m^3 (60%), 2.07*10^7 m^3 (48%), and 1.31*10^7 m^3 (30%).

In the RCP8.5 scenario (Figs. 8, 9), the glacier ice shrinks faster and ice volume is lost more rapidly than the RCP4.5 scenario. Specially, the east branch glacier shrinks to 0.99 km^2 (87%), 0.76 km^2 (66%), 0.44 km^2 (38%), 0.17 km^2 (15%), and 0.06 km^2 (5%) in 2010, 2030, 2050, 2070 and 2100. The ice volume shrinks to 5.30*10^7 m^3 (74%), 2.53*10^7 m^3 (36%), and 9.58*10^7 m^3 (13%), 3.65*10^7 m^3 (5.1%), 1.03*10^6 m^3 (1.4%) respectively. The west branch shrinks to 0.64 km^2 (88%), 0.51 km^2 (70%), 0.42 km^2 (57%), 0.36 km^2 (50%) and 0.31 km^2 (42%) in 2010, 2030, 2050, 2070 and 2100. The ice volume shrinks to 3.35*10^7 m^3 (77%), 1.87*10^7 m^3 (43%), 1.13*10^7 m^3 (26%), and 9.16*10^6 m^3 (21%), 8.00*10^6 m^3 (18%). Generally, in the scenario of RCP8.5, glacier retreats and shrinks much faster than RCP4.5.

West and east branches of glaciers have different responses to climate change. In 2050, comparing with 1980, the area of west branch glacier will shrink by 19–43% (the uncertainty is mainly caused by different climate scenarios), and ice volume will decrease by 40–74%. For the east branch, its glacier area will shrink by 21–62%, the volume will be reduced by 46–86%. In addition, in 2100, 39–58% area of west branch glacier will disappear, and 70–82% of ice volume will lose. While the glacier area of east branch will shrink by 45–95%, and the ice volume will lose 82–98.6%. Hence, the east branch retreats and shrinks much faster than its west neighbor, and the west branch glacier is probably to be larger than the east glacier in future. Although the east branch glacier has larger glacier area at present, it is facing a greater risk to disappear, probably due to its relatively low altitude. It is also interesting to find that the east branch glacier is probably further spited into two small glaciers which is likely impacted by the non-homogenous ice-thickness and the sub-glacier topography.

It is worthwhile to note that the Δ*h*-parameterization can only simulate the change of glacier area and elevation in the glacier retreat condition, instead of glacier advance. Therefore, the annual variation is not appropriate to be used as model input to update glacier surface elevation that is the reason we used every 5 years glacier variation to update the glacier elevation and surface area.

4.2.3. Tipping point of melting water supply

The melting water tipping point from the Urumqi Glacier No. 1 was predicted by the FLEX^G-Δh model in the climate scenarios of RCP4.5 and RCP8.5 from 2010 to 2100. We found that different climate change scenarios result in a large uncertainty while predicting the annual glacier runoff (Fig. 10). We are likely experiencing the tipping point of glacier melting, or will experience it around 2020. After the turning point, the runoff from glacier melting will experience a dramatic decrease from 2020 to 2050. From 2050 to the end of the 21st century, the glacier runoff will gradually decrease. These results are largely in line with previous modelling studies in the neighboring region (Sorg et al., 2014). These results alert us that immediate mitigation measures should be taken to adapt to this fast glacier change to assure long-term water security in this region.

5. Conclusions

In this study, we integrated a spatially distributed hydrological model (FLEX^G) and a glacier retreat model (Δh-parameterization) to assess the impact of climate change on glacier thinning, retreat, and its influence on hydrology and water resource. The coupled model (FLEX^G-Δh) was tested in the Urumqi Glacier No. 1 catchment with the longest and most comprehensive measurements in China. Besides, the model was validated by hydrological and glaciological data, including daily runoff, annual glacier mass balance (GMB), annual equilibrium line altitude (ELA), and the unusual historical glacier area maps in 1980, 1994, and 2002. The model satisfactorily reproduced hydrological processes and glacier variation, which illustrates the excellent applicability of this coupled model in the study catchment. Furthermore, we used the model to predict glacier variation and its impact on water resources by the end of 21st century, using the forcing data of two downscaled climate scenarios (RCP4.5 and RCP8.5) with bias correction from six empirical approaches. Results show that glacier area will lose up to a half (−54%) of their 1980 extent in 2050, and up to −80% in 2100; while ice volume will decrease up to −79% in 2050, and − 92% in 2100. The impact of the glacier retreat on downstream water supply was assessed by analyzing the tipping point of glacier melt, and the prediction show that the peak water will likely occur around 2020, and then reducing water supply will happen in this catchment. These results alert us that urgent mitigation measures are needed to adapt to this fast glacier change to assure long-term water security in this region.

Acknowledgement

Firstly, we would like to thank the great pioneers on glaciological studies in the Urumqi Glacier No. 1, who dedicated their lifelong energy to this arduous but glorious career. Without their tough work on the long-term field measurement, this paper can never happen. This study was supported by the National Key R&D Program of China (2017YFE0100700), the Key Program of National Natural Science Foundation of China (No. 41730646), and financially supported by the Key Laboratory for Mountain Hazards and Earth Surface Process, Institute of Mountain Hazards and Environment, Chinese Academy of Sciences (KLMHESP-17-02). We thank two anonymous reviewers for providing constructive comments, which greatly improved this manuscript.

Appendix A. Supplementary data

Supplementary data to this article can be found online at https://doi.org/10.1016/j.scitotenv.2018.07.004.

References

Beven, K., Binley, A., 1992. The future of distributed models: model calibration and uncertainty prediction. Hydrol. Process. 6:279–298. https://doi.org/10.1002/hyp.3360060305.

Bhutiyani, M.R., Kale, V.S., Pawar, N.J., 2008. Changing streamflow patterns in the rivers of northwestern Himalaya: implications of global warming in the 20th century. Curr. Sci. India. 95 (5), 618–626.

Ding, Y., Liu, S., Li, J., Shangguan, D., 2006. The retreat of glaciers in response to recent climate warming in western China. Ann. Glaciol. 43:97–105. https://doi.org/10.3189/172756406781812005.

Dong, Z., Qin, D., Ren, J., Li, K., Li, Z., 2012. Variations in the equilibrium line altitude of Urumqi glacier no. 1, Tianshan Mountains, over the past 50 years. Chin. Sci. Bull. 57:4776–4783. https://doi.org/10.1007/s11434-012-5524-1.

Duethmann, D., Peters, J., Blume, T., Vorogushyn, S., Güntner, A., 2014. The value of satellite-derived snow cover images for calibrating a hydrological model in snow-dominated catchments in Central Asia. Water Resour. Res. 50, 2002–2021.

Etter, S., Addor, N., Huss, M., Finger, D., 2017. Climate change impacts on future snow, ice and rain runoff in a Swiss mountain catchment using multi-dataset calibration. J. Hydrol. 13 (Supplement C):222–239. https://doi.org/10.1016/j.ejrh.2017.08.005.

Fujita, K., Sakai, A., 2014. Modelling runoff from a Himalayan debris-covered glacier. Hydrol. Earth Syst. Sci. 18:2679–2694. https://doi.org/10.5194/hess-18-2679-2014.

Gao, H., He, X., Ye, B., Pu, J., 2012. Modeling the runoff and glacier mass balance in a small watershed on the Central Tibetan Plateau, China, from 1955 to 2008. Hydrol. Process. 26:1593–1603. https://doi.org/10.1002/hyp.8256.

Gao, H., Ding, Y., Zhao, Q., Hrachowitz, M., Savenije, H.H.G., 2017a. The importance of aspect for modelling the hydrological response in a glacier catchment in Central Asia. Hydrol. Process. 31 (16):2842–2859. https://doi.org/10.1002/hyp.11224.

Gao, H., Han, T., Liu, Y., Zhao, Q., 2017b. Use of auxiliary data of topography, snow and ice to improve model performance in a glacier-dominated catchment in Central Asia. Hydrol. Res. 48, 1418 LP–1437.

Goodison, B., Louie, P., Yang, D., 1997. The WMO solid precipitation measurement intercomparison. World Meteorological Organization-Publications-WMO TD, pp. 65–70.

Gudmundsson, L., Tallaksen, L., Stahl, K., Clark, D.B., Dumont, E., Hagemann, S., et al., 2012. Comparing large-scale hydrological model simulations to observed runoff percentiles in Europe. J. Hydrometeorol. 13 (2), 604–620.

Gupta, H.V., Kling, H., Yilmaz, K.K., Martinez, G.F., 2009. Decomposition of the mean squared error and NSE performance criteria: implications for improving hydrological modelling. J. Hydrol. 377:80–91. https://doi.org/10.1016/j.jhydrol.2009.08.003.

Huss, M., Jouvet, G., Farinotti, D., Bauder, A., 2010. Future high-mountain hydrology: a new parameterization of glacier retreat. Hydrol. Earth Syst. Sci. 14:815–829. https://doi.org/10.5194/hess-14-815-2010.

Huss, M., Zemp, M., Joerg, P.C., Salzmann, N., 2014. High uncertainty in 21st century runoff projections from glacierized basins. J. Hydrol. 510:35–48. https://doi.org/10.1016/j.jhydrol.2013.12.017.

Immerzeel, W.W., van Beek, L.P.H., Bierkens, M.F.P., 2010. Climate change will affect the asian water towers. Science 328, 1382–1385 (80-).

Immerzeel, W.W., van Beek, L.P.H., Konz, M., Shrestha, A.B., Bierkens, M.F.P., 2012. Hydrological response to climate change in a glacierized catchment in the Himalayas. Clim. Chang. 110 (3):721–736. https://doi.org/10.1007/s10584-011-0143-4.

Kraaijenbrink, P.D.A., Bierkens, M.F.P., Lutz, A.F., Immerzeel, W.W., 2017. Impact of a global temperature rise of 1.5 degrees celsius on Asia's glaciers. Nature 549, 257–260.

Li, Z., Wang, W., Zhang, M., et al., 2010. Observed changes in streamflow at the headwaters of the Urumqi River, eastern Tianshan, central Asia. Hydrol. Process 24:217–224. https://doi.org/10.1002/hyp.7431.

Li, H., Ng, F., Li, Z., et al., 2012. An extended "perfect-plasticity" method for estimating ice thickness along the flow line of mountain glaciers. J. Geophys. Res. Earth Surf. 117 (n/a-n/a). https://doi.org/10.1029/2011JF002104.

Li, H., Beldring, S., Xu, C.-Y., et al., 2015. Integrating a glacier retreat model into a hydrological model – case studies of three glacierised catchments in Norway and Himalayan region. J. Hydrol. 527:656–667. https://doi.org/10.1016/j.jhydrol.2015.05.017.

Matthews, T., Hodgkins, R., Wilby, R.L., et al., 2015. Conditioning temperature-index model parameters on synoptic weather types for glacier melt simulations. Hydrol. Process. 29:1027–1045. https://doi.org/10.1002/hyp.10217.

Ming, J., Xiao, C., Du, Z., Yang, X., 2013. An overview of black carbon deposition in high Asia glaciers and its impacts on radiation balance. Adv. Water Resour. 55:80–87. https://doi.org/10.1016/j.advwatres.2012.05.015.

Pritchard, H.D., 2017. Asia's glaciers are a regionally important buffer against drought. Nature 545, 169–174.

Ren, Z., Gao, H., Elser, J.J., Zhao, Q., 2017. Microbial functional genes elucidate environmental drivers of biofilm metabolism in glacier-fed streams. Sci. Rep. 7, 12668. https://doi.org/10.1038/s41598-017-13086-9.

Schirmer, M., Wirz, V., Clifton, a., Lehning, M., 2011. Persistence in intraannual snow depth distribution: 1. Measurements and topographic control. Water Resour. Res. 47 (9) (n/a–n/a). https://doi.org/10.1029/2010WR009426.

Seibert, J., Jenicek, M., Huss, M., Ewen, T., 2015. Snow and ice in the hydrosphere. In: Haeberli, W., Whiteman, C. (Eds.), Snow and ice-related hazards, risks, and disasters. Elsevier, Amsterdam, pp. 99–130.

Seibert, J., Vis, M.J.P., Kohn, I., et al., 2017. Technical note: representing glacier dynamics in a semi-distributed hydrological model. Hydrol. Earth Syst. Sci. Discuss. 2017:1–20. https://doi.org/10.5194/hess-2017-158.

Wang, L., Sun, Litao, Shrestha, Maheswor, Li, Xiuping, Liu, Wenbin, Zhou, Jing, Yang, Kun, Lu, Hui, Chen, Deliang, 2016. Improving snow process modeling with satellite-based estimation of near-surface-air-temperature lapse rate. J. Geophys. Res.-Atmos. 121: 12005–12030. https://doi.org/10.1002/2016JD025506.

Seibert, J., 1997. Estimation of parameter uncertainty in the hbv model. Nord. Hydrol. 28, 247–262.

Sorg, A., Huss, M., Rohrer, M., Stoffel, M., 2014. The days of plenty might soon be over in glacierized central Asian catchments. Environ. Res. Lett. 9, 104018.

Tarasova, L., Knoche, M., Dietrich, J., Merz, R., 2016. Effects of input discretization, model complexity, and calibration strategy on model performance in a data-scarce glacierized catchment in Central Asia. Water Resour. Res. 52:4674–4699. https://doi.org/10.1002/2015WR018551.

Thayyen, R.J., Gergan, J.T., 2010. Role of glaciers in watershed hydrology: a preliminary study of a 'Himalayan catchment'. Cryosphere 4 (1):115–128. https://doi.org/10.5194/tc-4-115-2010.

Wang, L., Zhou, J., Qi, J., et al., 2017. Development of a land surface model with coupled snow and frozen soil physics. Water Resour. Res. 53:5085–5103. https://doi.org/10.1002/2017WR020451.

Yang, K., Koike, T., 2005. A general model to estimate hourly and daily solar radiation for hydrological studies. Water. Resour. Res. 41 (n/a-n/a). https://doi.org/10.1029/2005WR003976.

Yang, D., Jiang, T., Zhang, Y., Kang, E., 1988. Analysis and correction of errors in precipitation measurement at the head of Urumqi River, Tianshan. J. Glaciol. Geocryol. 10, 384–400.

Yang, D., Goodison, B., Metcalfe, J., Louie, P., Elomaa, E., Hanson, C., Lapin, M., 2001. Compatibility evaluation of national precipitation gage measurements. J. Geophys. Res. 106:1481–1491. https://doi.org/10.1029/2000jd900612.

Ye, B., Yang, D., Jiao, K., et al., 2005. The Urumqi River source Glacier No. 1, Tianshan, China: changes over the past 45 years. Geophys. Res. Lett. 32, L21504. https://doi.org/10.1029/2005GL024178.

Zhang, Y., Liu, S., Ding, Y., 2007. Glacier meltwater and runoff modelling, Keqicar Baqi glacier, southwestern Tien Shan, China. J. Glaciol. 53:91–98. https://doi.org/10.3189/172756507781833956.

Zhang, S., Ye, B., Liu, S., et al., 2012. A modified monthly degree-day model for evaluating glacier runoff changes in China. Part I: model development. Hydrol. Process. 26: 1686–1696. https://doi.org/10.1002/hyp.8286.

Zhang, T., Ju, L., Leng, W., et al., 2015. Thermomechanically coupled modelling for land-terminating glaciers: a comparison of two-dimensional, first-order and three-dimensional, full-stokes approaches. J. Glaciol. 61:702–712. https://doi.org/10.3189/2015JoG14J220.